Received: 13 November 2023 | Revised: 3 April 2024 | Accepted: 6 April 2024

DOI: 10.1002/rra.4287

SPECIAL ISSUE PAPER

WILEY

Vertical root profiles of grey alder (*Alnus incana*) trees growing in highly disturbed river environments

Matteo Stamer[1] | Angela M. Gurnell[2] | Walter Bertoldi[1,3]

[1]Department of Civil, Environmental and Mechanical Engineering, University of Trento, Trento, Italy

[2]School of Geography, Queen Mary University of London, London, UK

[3]Center Agriculture Food Environment, University of Trento, Trento, Italy

Correspondence
Walter Bertoldi, Department of Civil, Environmental and Mechanical Engineering, University of Trento, Via Mesiano, 77, 38123, Trento (TN), Italy.
Email: walter.bertoldi@unitn.it

Funding information
European Union; Italian Ministry of University and Research, Grant/Award Number: L232/2016

Abstract

The ability of plants to colonize the fluvial environment and withstand uprooting by floods is largely controlled by the anchoring effect of roots. We characterized the root architecture and tensile strength of *Alnus incana*, a riparian tree species of the Betulaceae family for which there are no systematic observations of its vertical root structure. Four *A. incana* individuals and two nearby *Populus nigra* 3–10 years old growing on bars in gravel-bed rivers were excavated. Their root structure was characterized in terms of root diameter, age, and depth and was related to sediment grain size and scour or deposition by floods. Root tensile strength was also measured as a function of root diameter using a load cell and displacement transducer attached to individual roots. The architecture of *A. incana* roots differed from that of nearby *P. nigra*, as all roots were in fine, sandy sediments, growing in one or more dense radial layers of which the most prominent was 0.2–0.3 m below the surface. The layers reflect deposition of fine sediments during floods. New fine sediment deposits promote the growth of a new root layer close to the aggraded ground surface. Root tensile strength was similar to Salicaceae species. These observations indicate that *A. incana* colonizes habitats that have already received fine sediment deposition, most likely induced by other young plants, especially Salicaceae species. *A. incana* then provides a high near-surface root biomass, potentially further stabilizing surfaces and playing a complementary role as an ecosystem engineer.

KEYWORDS
Alnus incana, biogeomorphology, *Populus nigra*, riparian vegetation, root reinforcement, root tensile strength, root vertical profile

1 | INTRODUCTION

Vegetation is one of the three main components, along with water and sediment, controlling the style and dynamics of fluvial systems (Gurnell et al., 2012; Gurnell et al., 2016). River ecosystems in temperate climates are disturbance dominated, where the ratio between vegetation resistance and flood disturbance is the critical parameter defining the potential for vegetation to grow and influence the river evolutionary trajectory (Corenblit et al., 2014). Floods can damage vegetation in several ways, including anoxia as a result of waterlogging, and direct physical damage from transported sediments, burial, and uprooting (Politti et al., 2018). Recent studies have highlighted that uprooting is the main cause of vegetation loss in gravel-bed rivers (Bankhead et al., 2017) and that uprooting occurs mainly in association with riverbed erosion (uprooting type II as defined by Edmaier et al., 2011, 2014). The drag exerted by the flow is generally not sufficient to uproot a plant, except in the very early stages (a few weeks to months) of the growth of a seedling (Bywater-Reyes et al., 2015; Calvani et al., 2019; Perona & Crouzy, 2018), indicating that root anchorage, including root strength, vertical structure, and depth, play a crucial role in the uprooting resistance of vegetation. Root density and individual root strength are also relevant parameters controlling

bank stability and erosion, adding cohesion to bank sediments (Abernethy & Rutherfurd, 2001; Andreoli et al., 2020; Pollen & Simon, 2005).

Despite their relevance, data on the vertical distribution of roots in riparian, highly disturbed environments are scarce. Conceptually, two idealized models are possible, depending on where roots find the main source of water as well as nutrients. In stable environments, with the formation of soil horizons that can store a significant amount of water as well as nutrients, plants develop predominantly near-surface roots, with a density that decreases downwards below the surface in an exponential profile (Schenk & Jackson, 2002). Riparian species such as those of the Salicaceae family (*Salix*, *Populus*) are typically phreatophytes and develop deeper roots that track the ground water table. In this case, the root vertical profile depends on the distance to the mean ground water table level and its seasonal and flood-related fluctuations (Tron et al., 2015). Pasquale et al. (2012, 2014) measured the vertical root structure of young *Salix* cuttings planted on gravel bars. They reported that the root profile depends mainly on the distance from the median groundwater level, with larger fractions of the root biomass on the upper (lower) part in the case of cuttings growing at low (high) elevation. Local conditions, in terms of flood disturbance and sediment grain size, can also affect the vertical root profile. Holloway et al. (2017a, 2017b, 2017c) showed that mature black poplar trees (*Populus nigra*) growing on river banks and islands show very complex root distributions, reflecting the local flood history and consequent bending, damage, and partial burial of the plants over the sequence of inundation events to which they have been exposed.

Recent studies have shown that trees located in different habitats across a gradient from relative shelter to increasing exposure to floods are characterized by different morphological and biomechanical traits, with stronger and deeper roots in areas more affected by flood disturbance (Hortobágyi et al., 2017). This means that different Salicaceae species may act as ecosystem engineers in different locations, taking advantage of their greater resistance to uprooting and/or higher above-ground biomass to induce enhanced fine sediment deposition (Hortobágyi et al., 2018). Similarly, field observations on the Tagliamento River (Italy) have shown that a member of the Betulaceae family, grey alder (*Alnus incana*) can also colonize bare riverine sediments and can complement the ecosystem engineering role of the dominant riparian tree species, *P. nigra* (Bertoldi & Gurnell, 2020). However, to our knowledge there is no systematic information available on the root architecture of *A. incana*, as compared to the more commonly studied Salicaceae species.

To fill this gap, we gathered field data to characterize the root strength and vertical root distribution of individual *A. incana* trees growing on bars in gravel-bed rivers and to explore the controls on root vertical profiles exerted by sediment grain size and flood disturbance. We also gathered data on nearby *P. nigra* trees to allow comparisons with a species whose roots have attracted greater research attention. These observations will contribute to enhancing mathematical models used to predict sediment root reinforcement and vegetation uprooting resistance within highly disturbed river environments.

2 | METHODS

During September to November 2020, we excavated four *A. incana* plants of different age in two gravel-bed rivers in north-east Italy (Figure 1a). In addition, we excavated two *P. nigra* plants growing close to and of similar age to two of the *A. incana* plants to allow for direct comparison of the root systems of individuals of the two species in the same environmental setting.

Two *A. incana* trees of about 10 years age were located along an island braided reach of the Tagliamento River, Italy (Figure 1b), in the same area investigated by Holloway et al. (2017a, 2017b, 2017c) and Bertoldi and Gurnell (2020). The Tagliamento River is a large gravel-bed river that is considered one of the most natural in the Alps, where many studies on biogeomorphic feedbacks between vegetation and fluvial morphology have been carried out (e.g., Bertoldi et al., 2011; Gurnell & Bertoldi, 2022; Gurnell & Petts, 2006; Gurnell et al., 2001). The reach has a median bed material grain size of about 40 mm, but with a significant proportion of sand, a longitudinal slope of about 0.003 m/m, a width of up to 1 km, and several established and pioneer islands, where *P. nigra* and *Salix* spp. are the most common species. *A. incana* occurs only sporadically in specific locations, such as along secondary channel edges (Bertoldi & Gurnell, 2020).

The other four investigated trees were located along the Centa Creek, a tributary of the Brenta River (north-east Italy) near the village of Caldonazzo (Trento Province) (Figure 1c). The Centa Creek is a gravel-bed river with a flashy hydrological regime, with major floods occurring during heavy convective rainfall events in autumn. Sediment production in the catchment is high, and in the downstream reaches the river has been extensively regulated with a series of 1–1.5 m high check dams spaced at approximately 100–200 m intervals, which limit sediment flux and reduce the slope from its natural value of 0.017 m/m. The river is also embanked, confining it to an active width of approximately 50 m. Vegetation colonizes the river bed extensively in the periods between floods, when the river frequently runs dry, encroaching large parts of the active channel where the morphology has been stabilized by the engineering works. *P. nigra* and *Salix* spp. are again dominant, with occasional *A. incana* plants. The vegetation is clear cut every 5–8 years to avoid complete encroachment. We selected a reach with extensive young trees, ranging in age from 3 to 5 years, to complement the older plants investigated along the Tagliamento.

The six trees were excavated by hand, carefully removing sediment to minimize root damage. We excavated to the deepest root and recorded the depth and diameter of the larger roots (diameter larger than 4 mm) and the size of the surrounding sediment. We did not recover the full length of lateral roots, but limited the analysis to an area of about 0.5 m radius around the tree's trunk, mapping the vertical distribution of the larger roots and the profile of the surrounding sediments. Tree and root ages were estimated by counting the number of annual growth rings in cores or cut trunks and roots, supported by analysis of aerial imagery to reconstruct when the relevant vegetated patches appeared at each site. *A. incana* tends to

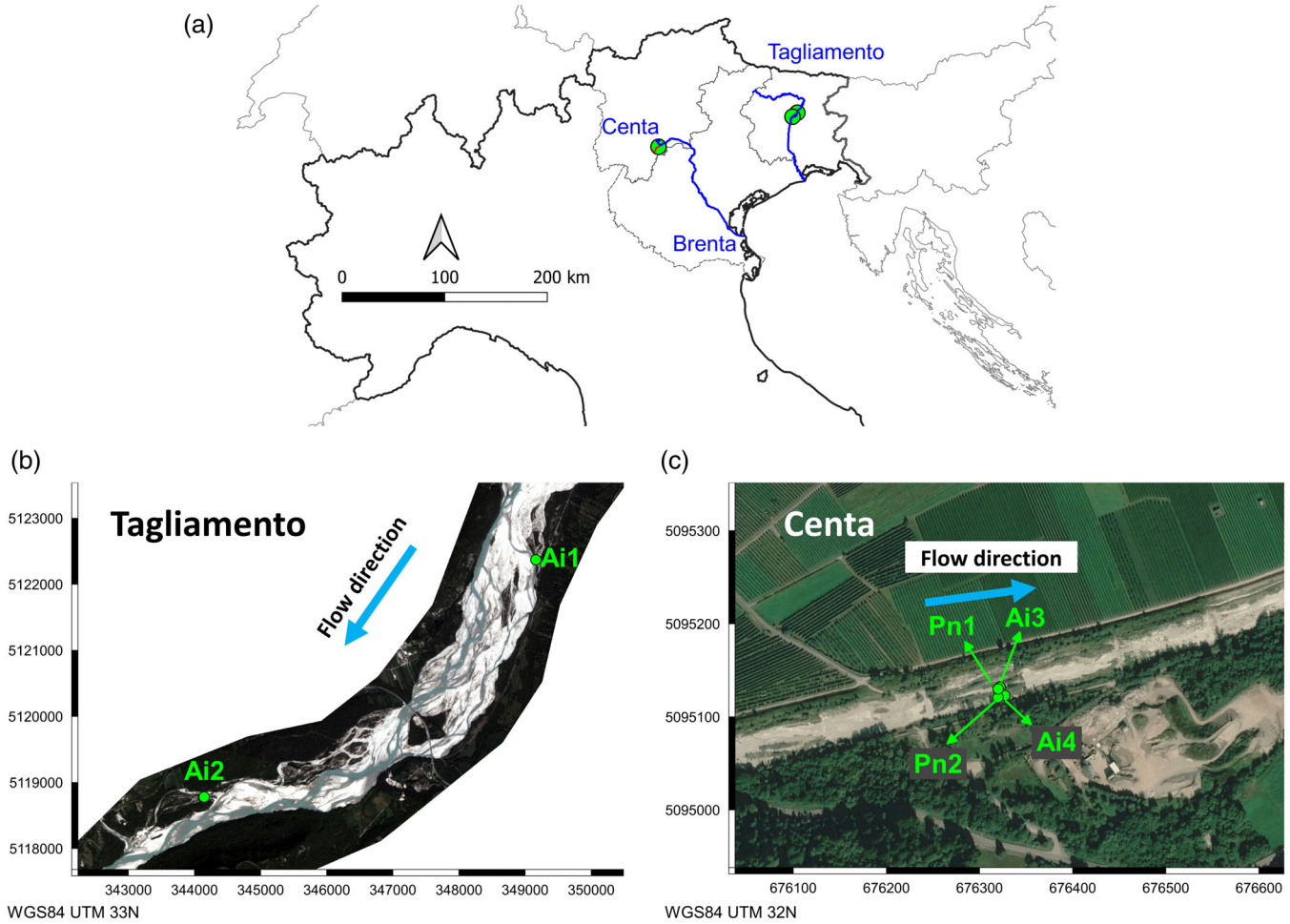

FIGURE 1 (a) Map of north Italy, with the location of the Tagliamento River and the Centa Creek, a small tributary of the Brenta River. (b) Satellite image of the Tagliamento reach, with location of the two excavated *A. incana* (© Planet, September 2020). (c) Aerial image of the Centa reach with the location of the four excavated trees, two *A. incana* and two *P. nigra* (© GoogleEarth, September 2019). [Color figure can be viewed at wileyonlinelibrary.com]

display false rings during periods of stress (e.g., droughts, floods), so our annual growth ring counts may be slight overestimates in some cases.

In addition, a sample of 135 pieces of finer *A. incana* roots (approximately 0.2 m long with diameters in the range 0.4–4 mm) was collected from the two sites. The tensile strength of each root specimen was tested using a load cell and displacement transducer attached to the root. Clamping devices used to connect each root to the load cell were selected to minimize root damage and avoid snapping at the clamping point. Once clamped, each root was subjected to increasing force until it snapped and the peak applied force was recorded, following Gurnell et al. (2019). Measurements were performed in the field, immediately after the roots were cut, and were repeated in the laboratory following several days of air-drying. The diameter of each root was calculated as the average of three measurements along the length of the root piece using an electronic caliper to an accuracy of 0.01 mm. Tensile strength was then computed as the ratio of peak resistance force to root cross-sectional area.

3 | RESULTS

The field observations on the four *A. incana* trees reveal a different architecture from the *P. nigra* trees located in the same environment.

The excavated *A. incana* individuals displayed one or more layers of horizontal roots, including a large number of fine roots, all located entirely in sand and finer sediments. No deep taproots were observed. Thus, all *A. incana* roots were contained in the sandy (deposited) layers and so were above the underlying gravel surface that presumably represents the original bar surface prior to finer sediment deposition. In the following, we qualitatively describe the vertical root structure of the four excavated *A. incana* trees. Summary information on each tree, including its height, trunk diameter at breast height, and estimated age are provided in Table 1.

Tree Ai1 was an isolated individual, 4.5 m tall and 7 years old, located on the top of a recently eroded bank (Figure 2a). All of the roots were in a layer of sand deposited on top of gravel. Most of the root biomass was close to the surface (0.2–0.3 m below the bank top surface), with roots arranged in a radial pattern but with more

larger roots on the upstream side of the tree (Figure 2b,c). The bank had been eroded within a year of the survey, before which the tree was part of a larger island bounded by an active and an abandoned channel. The bank top surface was approximately 1.5 m above the low flow water surface suggesting the groundwater table was probably more than 1 m below the tree's deepest root.

Tree Ai2 was the largest excavated *A. incana* individual, approximately 11 m tall and 10 years old. It was located on an island formed since 2008 in an area of the Tagliamento river that has experienced extensive vegetation encroachment and up to 1 m of fine sediment deposition during the last decade (Gurnell & Bertoldi, 2022). We exposed half of the root structure, on the side of the tree that was nearest a side channel. Ai2 displayed two main layers of larger lateral roots at approximately 0.55 m and 1.05 m below the ground surface. The first layer (around 0.55 m below the ground surface) was located within a recent sediment deposit (probably deposited during floods in autumn 2018 and 2019), with the trunk continuing downwards without any clear change in diameter (0.19 m) or structure (Figure 3a). Several large roots of up to 50 mm in diameter were present in this recently deposited layer, accompanied by numerous finer roots, particularly at approximately 0.2–0.3 m below the ground surface (Figure 3a). Below this upper root layer (Figure 3b) we excavated what was probably the previous trunk of the tree, with a smaller diameter (0.14 m) and a slight inclination in a downstream direction. A lower lateral root layer was present, approximately 0.5 m below the upper root layer and 1.05 m below the current ground surface. This layer was comprised of a smaller number of roots of larger average diameter than the upper layer (Figure 3b). All of the lateral roots were in sand, with a very thin layer of fine gravel separating the two root layers and the original gravel bar surface located about 0.25 m below the lower root layer.

Available topographic surveys (2010, 2013 and 2021, see Gurnell & Bertoldi, 2022 for further details) of the area within which Ai1 and Ai2 were located confirm that the site of Ai2 has been subject to more than 1 m of deposition in the last 10 years. Figure 4 reports the evolution of a transect through the location of Ai2 and across the ca. 12 m wide island on which it is located. The 2010 survey largely corresponds to the upper surface of a gravel layer which was exposed or excavated in the field in 2021. This is also confirmed by aerial images taken in 2009 and 2010, which show the area as a gravel bar with some sparse vegetation. The 2013 survey followed a large flood in November 2012 with a return interval of 15–20 years. This flood caused deposition of up to 0.4 m of sand and forms the layer in

TABLE 1 Diameter, height, and age of the six excavated trees.

ID	Diameter (mm)	Height (m)	Age (years)
Ai1	47	4.5	7
Ai2	140	11	10
Ai3	68	6	4
Ai4	19	2.4	3
Pn1	78	6.5	5
Pn2	32	1.8	2/3

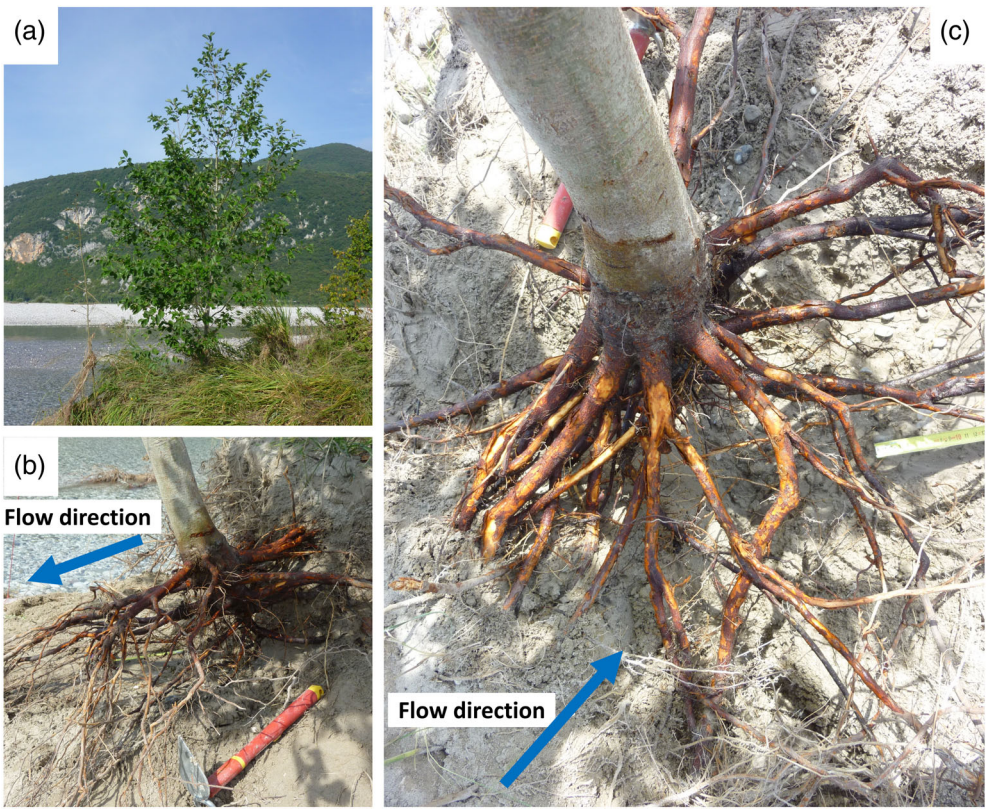

FIGURE 2 Photographs of tree Ai1: (a) before excavation; the excavated roots at late (b) and early (c) stages of excavation. [Color figure can be viewed at wileyonlinelibrary.com]

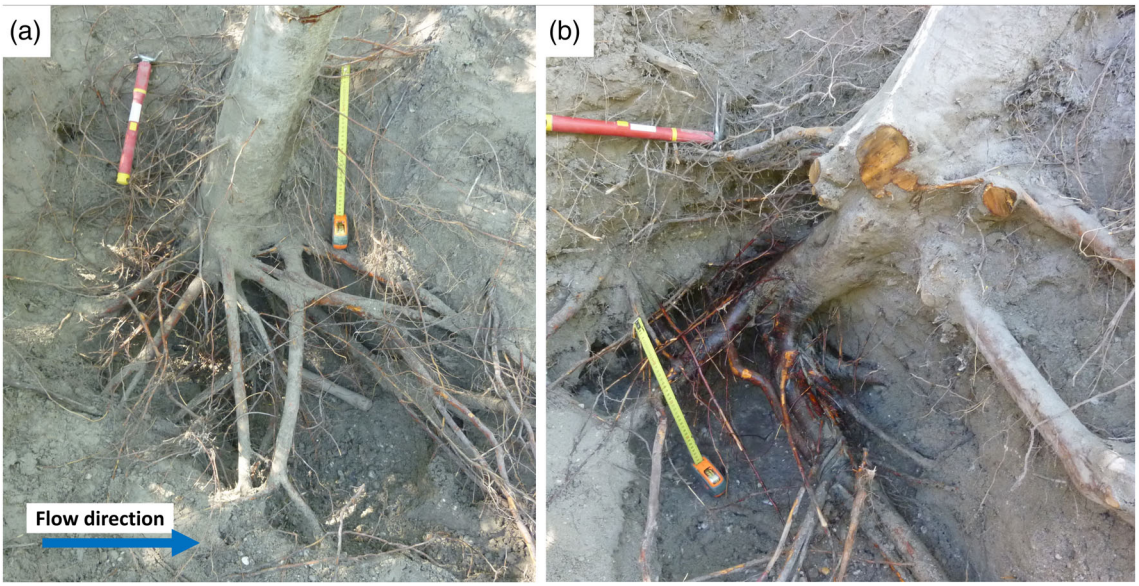

FIGURE 3 Photographs of tree Ai2: (a) the upper root layer about 0.6 m below the original soil level (brown mark at the top of the trunk); (b) the lower root layer, after cutting the upper root layer. [Color figure can be viewed at wileyonlinelibrary.com]

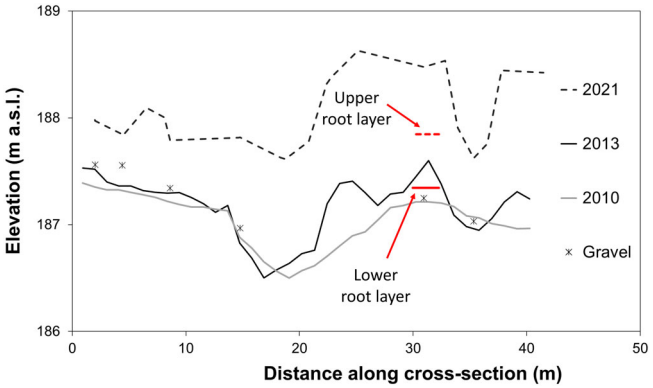

FIGURE 4 Reconstruction of bed elevation changes in comparison with the observed 2020 root profile of tree Ai2. The * symbols correspond to the upper limit of gravel deposits exposed during excavations in 2021. [Color figure can be viewed at wileyonlinelibrary.com]

which the lower lateral roots developed. This is also confirmed by an age estimate of 9 years for the large diameter roots within this lower layer. The upper layer of roots were estimated to be ca. 2–3 years younger than those in the lower layer, which corresponds with deposition of at least 0.4 m of sediment during a flood in November 2014. The 2021 topographic survey shows a total depositional depth of up to 1.2 m on the original gravel surface, with the most recent 0.5–0.6 m of deposition attributable to floods in autumn 2018 and 2019. Given that the channel to the left of the island in Figure 4 was dry at low flow in 2010, we estimate that the groundwater level is probably located at least 0.8 m below the deepest roots of Ai2.

Trees Ai3 and Ai4, excavated along the Centa creek, were younger than those excavated along the Tagliamento. Their root structures follow a similar pattern to Ai1 and Ai2. Both trees displayed two lateral root layers, the upper layer formed following deposition of fine sediment. Ai3 had an upper layer at 0.3 m below the ground surface with a lower layer located 0.5 m below the upper layer (Figure 5). Both layers displayed a radial pattern of lateral roots, but in this case with a larger proportion of the roots on the downstream side of the trees.

Tree Ai3, which was 4 years old, had 55 lateral roots greater than 4 mm in diameter (largest root was 21 mm diameter) radiating from the trunk. Of these, approximately 20 were concentrated within a 0.2 m vertical distance within each of the two layers and all roots were developed within sand deposits.

Tree Ai4 was the smallest (2.4 m) and youngest (3 years) of the four excavated *A. incana* trees. Excavation revealed that seven stems visible above ground originated from the same plant, and were probably the result of damage by a flood that occurred 2 years earlier (Figure 6). The flood deposited a sand layer approximately 0.5 m deep, through which the tree sprouted seven stems and formed an extensive layer of roots approximately 0.2 m below the ground surface. A lower root layer was located 0.5 m below this upper layer and immediately above a gravel surface. All the roots were in sand.

To directly compare the vertical root structure of *A. incana* with that of *P. nigra* individuals of similar age and dimensions and at the same location, we excavated two *P. nigra* trees, Pn1 and Pn2, located a short distance from Ai3 and Ai4, respectively (Figure 1c and Table 1).

Figure 7 shows the excavated root structures of trees Pn1 and Pn2. Three major differences were observed in their root structures when compared to those of nearby *A. incana*. First, both *P. nigra* plants had a main taproot that continued vertically into the gravel layer and accounted for a large proportion of the root biomass. Second, and particularly for Pn2, most of the roots were in gravel. Pn1 roots were in a mixture of sand and gravel, with a greater density of roots in

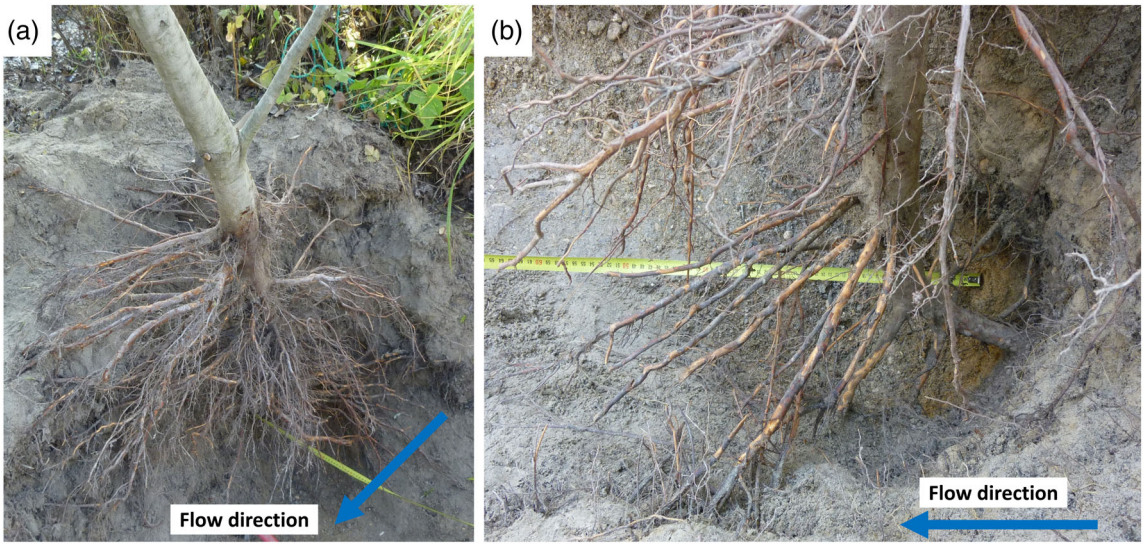

FIGURE 5 Photographs of tree Ai3: (a) the excavated roots; (b) the lower root layer, displaying more roots on the upstream side of the tree. [Color figure can be viewed at wileyonlinelibrary.com]

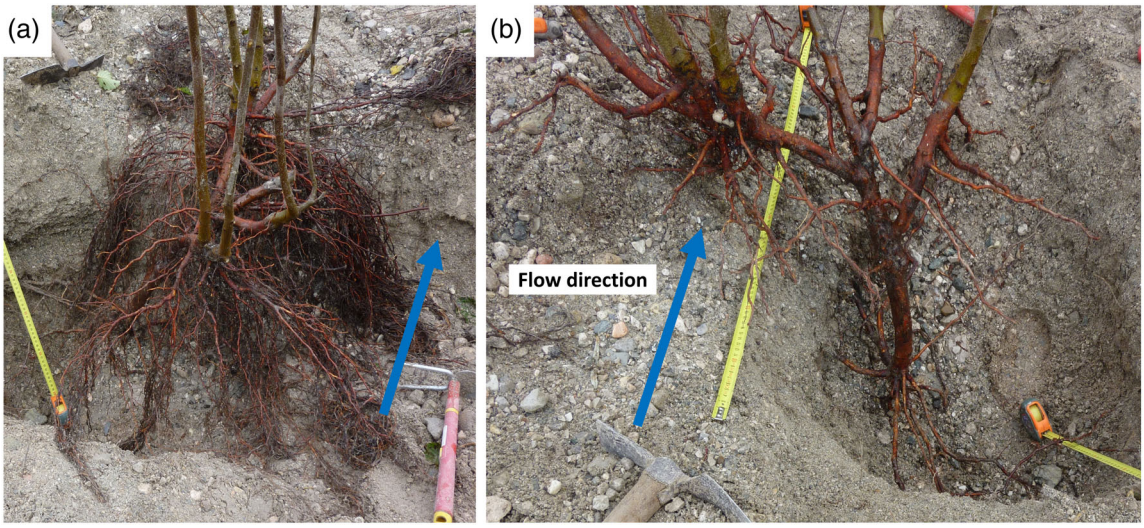

FIGURE 6 Photographs of tree Ai4: (a) the excavated roots; (b) the coarser root architecture (after removing all of the finer roots), with the lower root layer clearly visible. [Color figure can be viewed at wileyonlinelibrary.com]

the sandy layers. Third, the biomass of lateral roots and of fine roots was much lower when compared to the nearby, excavated *A. incana*. This was particularly noticeable for Pn2, which had only a few small (but >4 mm diameter) lateral roots and almost no fine roots. Pn2 grew on a gravel deposit, with finer sediments only at the base of the roots and close to the groundwater table. Pn1 had 4 larger horizontal roots (diameter approximately 30 mm), one on top of the other and oriented in the same direction (toward the bank, see enlargement in Figure 7a).

The vertical distribution of the horizontal area occupied by the roots of each excavated tree was computed from the sum of their cross-sectional areas within 0.1 m depth increments (Figure 8). All four *A. incana* trees present distinct layers of horizontal roots, with three trees (Ai1, Ai3, Ai4) displaying an upper layer within 0.2–0.3 m of the ground surface. Tree Ai2 was an exception in not having a distinct larger lateral root layer close to the surface, but this may be due to recent sediment deposition since some small, finer roots were present where such a root layer might be expected. Where lower lateral root layers are present (Ai2, Ai3, Ai4), they are always located within flood deposits, which, based on associations between larger root ages and flood dates, created new surface layers of finer sediments that were quickly penetrated by new roots. In contrast, the two *P. nigra* trees display a smaller horizontal root area that, in the case of Pn2 is almost an order of magnitude smaller than that of the nearby *A. incana*. This difference is even greater if the abundance of fine roots is considered, which were numerous for all the four

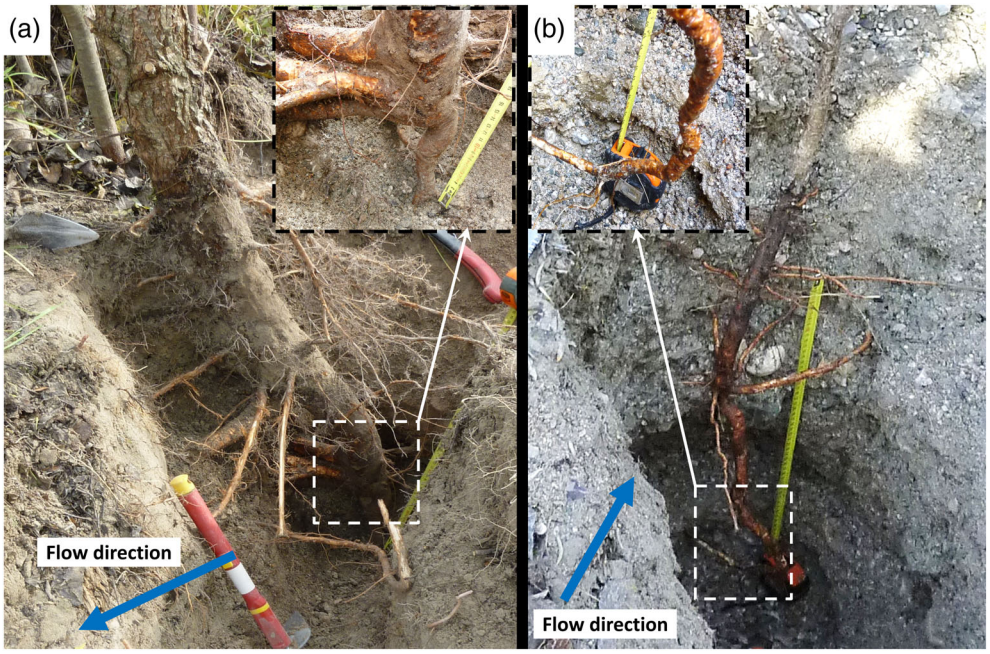

FIGURE 7 (a) A photograph of the excavated roots of tree Pn1, with an enlargement of the four larger horizontal roots and the taproot; (b) a photograph of the excavated roots of Pn2, with an enlargement of the taproot. [Color figure can be viewed at wileyonlinelibrary.com]

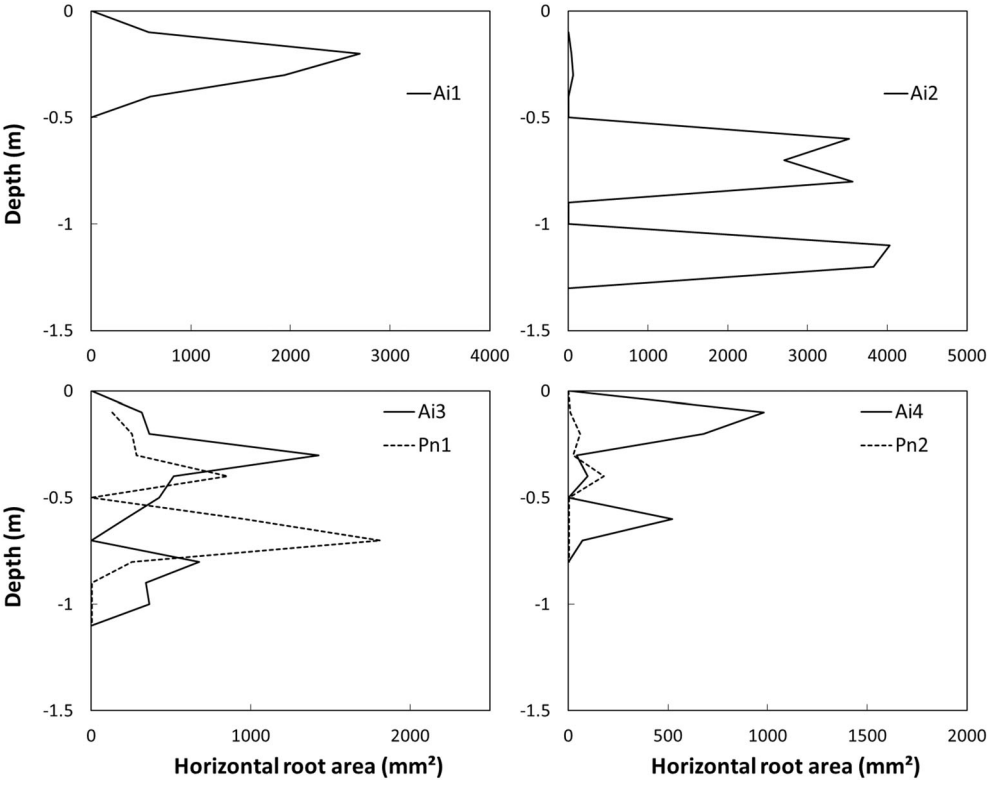

FIGURE 8 Vertical distributions of horizontal root area displayed by the six excavated trees.

A. incana and sparse or almost absent in the case of Pn1 and Pn2, respectively.

The tensile strength of the 135 *A. incana* roots measured in the field (living) and after several days of air drying in the laboratory (dried) show considerable scatter but with the highest values (up to 40 MPa) observed for smaller roots (diameter less than 1 mm) (Figure 9a). However, there was no statistically significant relationship between tensile strength and diameter, with the linear model estimated on log-transformed variables indicating a constant value of approximately 15 MPa regardless of root diameter. Dry roots showed a higher average tensile strength of approximately 20 MPa but once again, there was no statistically significant association between tensile strength and root diameter. Comparison with previously published data for *P. nigra* roots (Gurnell et al., 2019) showed generally similar

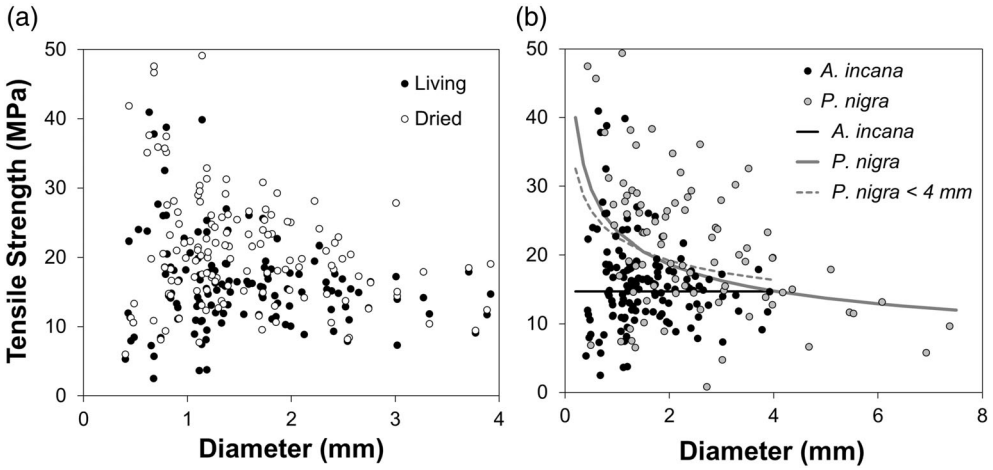

FIGURE 9 Observations and statistically significant power relationships between tensile strength and root diameter for (a) living and dried roots of *A. incana* and (b) living roots of *P. nigra* and *A. incana*.

values of tensile strength, with *P. nigra* roots showing only slightly higher values, but *P. nigra* roots showed a significant decrease in tensile strength with increasing root diameter.

4 | DISCUSSION

Our observations show that the root architecture of two young (3 and 4 years) *A. incana* trees differs significantly from that of two young (2 or 3 years and 5 years) *P. nigra* growing in close proximity and thus subject to similar environmental conditions. Furthermore, the root architecture of two older (7 and 10 years) *A. incana* trees growing at a different site and in a different environmental setting, show many similar characteristics to the two younger trees. Two main differences are relevant for understanding the processes leading to establishment and uprooting of *A. incana*: (i) all the roots we excavated were in fine, sandy sediments, although the two rivers are gravel-bed rivers; and (ii) *A. incana* roots grow predominantly near the surface, in dense radial layers located (initially) 0.2–0.3 m below the surface. Subsequent deposition of fine sediments promotes the growth of new root layers close to the new surface. Therefore, the four excavated *A. incana* did not send vertical roots into the underlying gravel layers and toward the water table. This suggests that this species mainly uses rainwater or floodwater that has percolated from the surface and been retained in the unsaturated finer sediment layers. The root structure of *A. incana* can be compared with that of *P. nigra*, as directly observed in two trees growing a short distance from two of the excavated *A. incana*. The two older Ai individuals can also be compared with previous measurements of *P. nigra* individuals reported by Holloway et al. (2017a, 2017b). In general, the younger *P. nigra* individuals observed in the present study had a deep taproot and a very small number of lateral roots, with a highly variable vertical distribution. The two older *A. incana* individuals were of similar age to the eight *P. nigra* individuals described by Holloway et al. (2017a, 2017b). Once again, all *P. nigra* individuals had a deep tap root that clearly differentiated them from Ai1 and Ai2, but they displayed many more and larger lateral roots than the younger *P. nigra* individuals excavated in the present study. These *P. nigra* lateral roots described by Holloway et al. (2017a, 2017b) were arranged in layers that corresponded to finer sediments deposited by past floods but they were less numerous than observed in association with *A. incana* in the present study. Furthermore, Holloway et al. (2017c) observed increased numbers of finer and coarser *P. nigra* roots associated with finer sediment layers, indicating that root layers in both species display vertical profiles that reflect the specific history of each excavated tree and its response to damage, erosion, and sediment deposition by floods.

Data on individual *A. incana* trees are scarce in the literature. However, recently, Andreoli et al. (2020) reported the vertical root distribution measured in seven trenches along two gravel bed rivers in South Tyrol (Italy). The study reports aggregate data on seven vertical root profiles excavated to a depth of 1 m, five on the Mareit River and two on the Ahr River. These profiles represented river banks colonized by *Alnus incana*, *Salix* spp. (mainly *S. eleagnos*, *S. purpurea*), *Betula pendula*, *Larix decidua*, *Fraxinus excelsior*, and *Picea abies*. Root area ratios were measured at 0.1 m intervals from the surface to a depth of 1 m at all sites. Three sites, one on the Mareit River and two on the Ahr River showed a high *A. incana* cover (over 80%), two sites on the Mareit river showed intermediate *A. incana* cover (43%, 53%), and the remaining two sites on the Mareit river showed negligible *A. incana* cover (0%, 16%). The two sites on the Ahr River were located in relatively mature, floodplain woodland. They showed root area ratios that were around four times higher than the other five sites, but this probably reflects site age as much as species composition. More importantly, they showed two peaks in root area ratio with increasing depth, the first within 0.25 m of the surface and the second between 0.55 and 0.65 m below the surface. On average the five young sites on the Mareit River showed lower average root area ratios and a progressive decline in root area ratio with depth below 0.25 m. When the profiles for the five sites are compared, those with negligible *A. incana* cover and dominated by *Salix* spp. show a more even root area ratio with a gradual decline with depth below 0.35 m; those with intermediate cover and a similar cover of *Salix* spp. show a very rapid decline in root area ratio to low values below 0.35 m; and the site dominated by *A. incana* also shows a rapid decline below

0.35 m but the decline plateaus to 0.65 m depth before dropping to similarly low values to the intermediate cover sites. Accepting that the research methods and locations used in our two studies were very different, the vertical root distributions observed by Andreoli et al. (2020) provide complementary evidence of abrupt changes in the root area ratio including multiple lateral root layers in association with *A. incana*.

Our measurements of the tensile strength of *A. incana* roots showed slightly higher values than those reported in previous studies of riparian species (Andreoli et al., 2020; Gurnell et al., 2019), and our measurements did not show a statistically significant trend with root diameter, in contrast to measurements for *P. nigra* and *Salix alba* (Gurnell et al., 2019) and a mix of roots from riparian species (predominantly *Salix* spp. and *A. incana*) reported by Andreoli et al. (2020). Gurnell et al. (2019) showed generally lower tensile strength for the two Salicaceae species investigated than our *A. incana* observations, which may explain the lower values of tensile strength reported by Andreoli et al. (2020) for their mixed (predominantly *Salix* spp. and *A. incana*) roots.

Root architecture and tensile strength are the two main components for estimating root reinforcement of sediment profiles (Pollen & Simon, 2005). The shallower root profile of *A. incana* when compared with the Salicaceae in the present research is supported by previous observations of *P. nigra* root profiles on the Tagliamento River (Holloway et al., 2017a, 2017b, 2017c) and by the observations of mixed root profiles from the Mareit and Ahr (Andreoli et al., 2020). The shallower root profile of *A. incana* may determine a sharp decrease in added cohesion and reinforcement with depth, limiting bank stability and resistance to lateral erosion. However, the dense radial surface root layer of *A. incana* could play a significant role in limiting the initiation of sediment transport at the surface, which could be particularly important if, as we observed, *A. incana* roots are confined to fine sediments. Considering that uprooting of riparian trees mainly occurs in association with significant erosion that exposes a large proportion of roots (Bywater-Reyes et al., 2015; Calvani et al., 2019), a root biomass concentrated in a near-surface layer may increase plant stability when erosion is shallow but is likely to have a limited effect in the case of deep scouring events such as may occur during lateral bank erosion. This also raises the question of the role of any secondary root layers, and whether much older individuals than those excavated in our study may support several deeper root layers and also greater lateral extension in their larger lateral roots. All of these observed or inferred properties of *A. incana* root architecture, including the large number of lateral roots and also the apparently higher root tensile strength of this species, could provide physical protection to an eroding bank once the roots become exposed. Such a process, where exposed roots remain to cover a significant proportion of the bank face and limit the mobilization of sediment, could have a similar effect to the cohesive slump blocks modeled by Eke et al. (2014). It would be also interesting to measure the uprooting (pull-out) resistance of *A. incana* seedlings when the root biomass is still low. Comparisons with the uprooting resistance of Salicaceae seedlings (uprooting type 1 sensu Edmaier et al., 2011) would establish the relative potential of *A. incana* to survive early flow disturbances and contribute to initial colonization of exposed riverine sediments. Early development of a radial root layer by *A. incana* seedlings could, at least partly, counteract the shallow root depth, as highlighted by Piqué et al. (2020), who compared the pull-out resistance of nine different riparian species typical of Chilean rivers.

Our observations of root strength and architecture confirm that *A. incana* is likely to have a different, complementary engineering role in gravel bed rivers where the dominant riparian species are from the Salicaceae family, extending the differences among Salicaceae species described by Hortobágyi et al. (2018). Our previous observations that *A. incana* tends to germinate and grow in less disturbed areas, especially along the margins of small side channels between vegetated islands (Bertoldi & Gurnell, 2020) and our observation in the present study that it develops in fine sediment deposits, suggests that it can only colonize habitats that have already been modified by previous vegetation colonization (e.g., by Salicaceae). Its presence may enhance the engineering effect of the Salicaceae by providing high root density at shallower depths, thereby enhancing the added cohesion from roots in the surface sediment layers. In addition, the combination of *A. incana* with Salicaceae species, increasing the richness of woody species present, could increase total root length and the number of root tips and thus reduce erosion rates, as observed for herbaceous plants by Allen et al. (2016). *A. incana* is a plant that can fix nitrogen through symbiosis with the nitrogen-fixing bacterium *Frankia alni* and so could have additional benefits for other plant species.

Our findings on the root structure of *A. incana*, with its dense shallow root biomass and potential to develop more than one layer of lateral roots, improves our understanding of plant growth strategies and demonstrates that root architecture is a key element in recognizing and interpreting fluvial biogeomorphic interactions. Our observations complement those of Hortobágyi et al. (2017), who reported differences in morphological and biomechanical traits of *P. nigra* according to their position on a gravel bar. They observed finer and more superficial roots at the bar tail, and deeper and stronger roots at the upstream-facing part of the bar. Hortobágyi et al. (2017) suggested that these contrasts could be due to differences in the magnitude of flow disturbances, which decrease downstream along the bar. However, there could also be an effect of grain size, as the bar tail was richer in sand. Indeed, disturbance, sediment type, and vegetation development are strongly linked, and more data are needed to better understand and disentangle feedbacks, particularly when roots are taken into account.

Despite recent advances, our ability to predict the vertical root profile of riparian trees in highly disturbed environments remains limited. Holloway et al. (2017a) concluded that moisture, grain size, and depth could only explain 36% and 26% of the variability in *P. nigra* root density and root area ratio, respectively. Mathematical models such as that proposed by Tron et al. (2014, 2015) proved to be valid in describing the vertical distribution of roots of phreatophytic plants as a function of the temporal fluctuations of the groundwater level. More recently, Perona et al. (2022) assembled three analytical root distribution models and developed an integrated framework that considers the

vertical and horizontal distribution of roots as a function of groundwater level and precipitation. This framework has the ability to model a range of different environmental conditions and vegetation species. However, the model does not consider grain size variability, nor the effect of bed surface morphological changes, such as scour and deposition, two variables that seem to have a notable effect on the trees that we excavated. The availability of more data (and more species, as reported here for *A. incana*) may help to improve predictive models and derive sets of parameters that can be used for different species. Recent, novel numerical (Caponi & Siviglia, 2018; Caponi et al., 2020) and stochastic models (Bau' et al., 2021) have been proposed to take into account the effects of different root profiles, demonstrating that roots play a crucial role in fluvial biogeomorphic feedbacks and can significantly influence the evolution of the river bed, but such models need to be informed by a larger body of field observations.

5 | CONCLUSIONS

We explored the root architecture and root tensile strength of *A. incana* growing on bars along two gravel-bed rivers in Northern Italy. Our field observations show that *A. incana* root growth strategy is different from that of the Salicaceae, such as *P. nigra*, which show a (deep) taproot and a vertical distribution that is strongly influenced by water table depth. Based on our observations, *A. incana* roots grow only in fine, sandy sediments and do not have a deep taproot. Their vertical root structure is independent of groundwater depth, with a dense layer of horizontal roots growing near the surface, typically at about 0.2–0.3 m depth. Deeper root layers are present when the tree has experienced fine sediment deposition. Several of the investigated individuals showed a second, deeper layer marking the position of the original riverbed surface and then a shallow layer formed closer to the current bed surface. The lack of a tap root indicates that *A. incana* is not a phreatophytic species and its vertical root distribution is not determined by the dynamics of the water table.

Data on the vertical root architecture of riparian species and a better understanding of the processes and parameters that control their biomass and vertical distribution are key to improving predictive biogeomorphic models, where the uprooting process is mainly controlled by root depth. The superficial but dense root structure of *A. incana* can significantly stabilize the upper layers of fine sediments, providing additional cohesion and direct physical protection covering a large part of exposed river banks. A shallow root structure may be less effective in limiting plant uprooting where deep scour occurs, as in the case of bank erosion at bends. Overall, *A. incana* is likely to play a complementary ecosystem engineering role along a river dominated by deeper rooted Salicaceae species, both in terms of its spatial position in less disturbed habitats where fine sediments have been deposited, and its vertical root profile, which adds a significant amount of biomass in the more superficial sediment layers. Future research, building on the data set and results presented here, will incorporate a wider range of riparian environmental settings and tree ages and will help to further develop these concepts.

ACKNOWLEDGMENTS

The authors thank the referees for their constructive comments and suggestions. WB acknowledges funding by the European Union under Next Generation EU, PRIN 2022 PNRR Prot. n. P20229WTX7 (project Green Rivers) and by the Italian Ministry of University and Research (MUR), in the framework of the project DICAM-EXC (Departments of Excellence 2023-2027, grant L232/2016).

CONFLICT OF INTEREST STATEMENT

The authors declare no conflicts of interest.

DATA AVAILABILITY STATEMENT

The data that support the findings of this study are available from the corresponding author upon reasonable request.

ORCID

Angela M. Gurnell https://orcid.org/0000-0002-7249-8202
Walter Bertoldi https://orcid.org/0000-0003-1158-2379

REFERENCES

Abernethy, B., & Rutherfurd, I. D. (2001). The distribution and strength of riparian tree roots in relation to riverbank reinforcement. *Hydrological Processes*, *15*(1), 63–79. https://doi.org/10.1002/hyp.152

Allen, D. C., Cardinale, B. J., & Wynn-Thompson, T. (2016). Plant biodiversity effects in reducing fluvial erosion are limited to low species richness. *Ecology*, *97*, 17–24. https://doi.org/10.1890/15-0800.1

Andreoli, A., Chiaradia, E. A., Cislaghi, A., Bischetti, G. B., & Comiti, F. (2020). Roots reinforcement by riparian trees in restored rivers. *Geomorphology*, *370*, 107389. https://doi.org/10.1016/j.geomorph.2020.107389

Bankhead, N. L., Thomas, R. E., & Simon, A. (2017). A combined field, laboratory and numerical study of the forces applied to, and the potential for removal of, bar top vegetation in a braided river. *Earth Surface Processes and Landforms*, *42*(3), 439–459. Portico. https://doi.org/10.1002/esp.3997

Bau', V., Borthwick, A. G. L., & Perona, P. (2021). Plant roots steer resilience to perturbation of river floodplains. *Geophysical Research Letters*, *48*(9), e2021GL092388. https://doi.org/10.1029/2021GL092388

Bertoldi, W., & Gurnell, A. M. (2020). Physical engineering of an Island-braided river by two riparian tree species: Evidence from aerial images and airborne lidar. *River Research and Applications*, *36*, 1183–1201. https://doi.org/10.1002/rra.3657

Bertoldi, W., Gurnell, A. M., & Drake, N. A. (2011). The topographic signature of vegetation development along a braided river: Results of a combined analysis of airborne lidar, colour air photographs and ground measurements. *Water Resources Research*, *47*(6), W06525. https://doi.org/10.1029/2010WR010319

Bywater-Reyes, S., Wilcox, A. C., Stella, J. C., & Lightbody, A. F. (2015). Flow and scour constraints on uprooting of pioneer woody seedlings. *Water Resources Research*, *51*, 9190–9206. https://doi.org/10.1002/2014WR016641

Calvani, G., Francalanci, S., & Solari, L. (2019). A physical model for the uprooting of flexible vegetation on river bars. *Journal of Geophysical Research: Earth Surface*, *124*(4), 1018–1034. https://doi.org/10.1029/2018JF004747

Caponi, F., & Siviglia, A. (2018). Numerical modeling of plant root controls on gravel bed river morphodynamics. *Geophysical Research Letters*, *45*(17), 9013–9023. https://doi.org/10.1029/2018GL078696

Caponi, F., Vetsch, D. F., & Siviglia, A. (2020). A model study of the combined effect of above and below ground plant traits on the ecomorphodynamics of gravel bars. *Scientific Reports*, *10*(1), 17062. https://doi.org/10.1038/s41598-020-74106-9

Corenblit, D., Steiger, J., González, E., Gurnell, A. M., Charrier, G., Darrozes, J., Dousseau, J., Julien, F., Lambs, L., Larrue, S., Roussel, E., Vautier, F., & Voldoire, O. (2014). The biogeomorphological life cycle of poplars during the fluvial biogeomorphological succession: A special focus on *Populus nigra* L. *Earth Surface Processes and Landforms*, *39*, 546–563. https://doi.org/10.1002/esp.3515

Edmaier, K., Burlando, P., & Perona, P. (2011). Mechanisms of vegetation uprooting by flow in alluvial non-cohesive sediment. *Hydrology and Earth System Sciences*, *15*(5), 1615–1627. https://doi.org/10.5194/hess-15-1615-2011

Edmaier, K., Crouzy, B., Ennos, R., Burlando, P., & Perona, P. (2014). Influence of root characteristics and soil variables on the uprooting mechanics of *Avena sativa* and *Medicago sativa* seedlings. *Earth Surface Processes and Landforms*, *39*(10), 1354–1364. https://doi.org/10.1002/esp.3587

Eke, E., Parker, G., & Shimizu, Y. (2014). Numerical modeling of erosional and depositional bank processes in migrating river bends with self-formed width: Morphodynamics of bar push and bank pull. *Journal of Geophysical Research: Earth Surface*, *119*, 1455–1483. https://doi.org/10.1002/2013JF003020

Gurnell, A. M., & Bertoldi, W. (2022). The impact of plants on fine sediment storage within the active channels of gravel-bed rivers: A preliminary assessment. *Hydrological Processes*, *36*(7), e14637. https://doi.org/10.1002/hyp.14637

Gurnell, A. M., Bertoldi, W., & Corenblit, D. (2012). Changing river channels: The roles of hydrological processes, plants and pioneer fluvial landforms in humid temperate, mixed load, gravel bed rivers. *Earth-Science Reviews*, *111*, 129–141. https://doi.org/10.1016/j.earscirev.2011.11.005

Gurnell, A. M., Corenblit, D., García de Jalón, D., González del Tánago, M., Grabowski, R. C., O'Hare, M. T., & Szewczyk, M. (2016). A conceptual model of vegetation–hydrogeomorphology interactions within river corridors. *River Research and Applications*, *32*(2), 142–163. https://doi.org/10.1002/rra.2928

Gurnell, A. M., Holloway, J. V., Liffen, T., Serlet, A. J., & Zolezzi, G. (2019). Plant root and rhizome strength: Are there differences between and within species and rivers? *Earth Surface Processes and Landforms*, *44*(1), 389–392. https://doi.org/10.1002/esp.4499

Gurnell, A. M., & Petts, G. E. (2006). Trees as riparian engineers: The Tagliamento River, Italy. *Earth Surface Processes and Landforms*, *31*, 1558–1574. https://doi.org/10.1002/esp.1342

Gurnell, A. M., Petts, G. E., Hannah, D. M., Smith, B. P. G., Edwards, P. J., Kollmann, J., Ward, J. V., & Tockner, K. (2001). Riparian vegetation and island formation along the gravel-bed Fiume Tagliamento, Italy. *Earth Surface Processes and Landforms*, *26*(1), 31–62. https://doi.org/10.1002/1096-9837(200101)26:1<31::AID-ESP155>3.0.CO;2-Y

Holloway, J. V., Rillig, M. C., & Gurnell, A. M. (2017a). Physical environmental controls on riparian root profiles associated with black poplar (*Populus nigra* L.) along the Tagliamento River, Italy. *Earth Surface Processes and Landforms*, *42*, 1262–1273. https://doi.org/10.1002/esp.4076

Holloway, J. V., Rillig, M. C., & Gurnell, A. M. (2017b). Underground riparian wood: Buried stem and coarse root structures of black poplar (*Populus nigra* L.). *Geomorphology*, *279*, 188–198. https://doi.org/10.1016/j.geomorph.2016.08.002

Holloway, J. V., Rillig, M. C., & Gurnell, A. M. (2017c). Underground riparian wood: Reconstructing the processes influencing buried stem and coarse root structures of black poplar (*Populus nigra* L.). *Geomorphology*, *279*, 199–208. https://doi.org/10.1016/j.geomorph.2016.07.027

Hortobágyi, B., Corenblit, D., Ding, Z., Lambs, L., & Steiger, J. (2017). Above- and belowground responses of *Populus nigra* L. to mechanical stress observed on the Allier River, France. *Géomorphologie: Relief, Processus, Environnement*, *23*(3), 219–231. https://doi.org/10.4000/geomorphologie.11748

Hortobágyi, B., Corenblit, D., Steiger, J., & Peiry, J. L. (2018). Niche construction within riparian corridors. Part I: Exploring biogeomorphic feedback windows of three pioneer riparian species (Allier River, France). *Geomorphology*, *305*, 94–111. https://doi.org/10.1016/j.geomorph.2017.08.048

Pasquale, N., Perona, P., Francis, R., & Burlando, P. (2012). Effects of streamflow variability on the vertical root density distribution of willow cutting experiments. *Ecological Engineering*, *40*, 167–172. https://doi.org/10.1016/j.ecoleng.2011.12.002

Pasquale, N., Perona, P., Francis, R., & Burlando, P. (2014). Above-ground and below-ground Salix dynamics in response to river processes. *Hydrological Processes*, *28*(20), 5189–5203. https://doi.org/10.1002/hyp.9993

Perona, P., & Crouzy, B. (2018). Resilience of riverbed vegetation to uprooting by flow. *Proceedings of the Royal Society A*, *474*, 20170547. https://doi.org/10.1098/rspa.2017.0547

Perona, P., Flury, R., Barry, D. A., & Schwarz, M. (2022). Tree root distribution modelling in different environmental conditions. *Ecological Engineering*, *185*, 106811. https://doi.org/10.1016/j.ecoleng.2022.106811

Piqué, G., Mao, L., & Becerra, P. (2020). Resistance to pull-out of Chilean riverine species: Evidence from laboratory experiments. *Geomorphology*, *361*, 107205. https://doi.org/10.1016/j.geomorph.2020.107205

Pollen, N., & Simon, A. (2005). Estimating the mechanical effects of riparian vegetation on stream bank stability using a fiber bundle model. *Water Resources Research*, *41*(7), W07025. https://doi.org/10.1029/2004WR003801

Politti, E., Bertoldi, W., Gurnell, A., & Henshaw, A. (2018). Feedbacks between the riparian Salicaceae and hydrogeomorphic processes: A quantitative review. *Earth-Science Reviews*, *176*, 147–165. https://doi.org/10.1016/j.earscirev.2017.07.018

Schenk, H. J., & Jackson, R. B. (2002). The global biogeography of roots. *Ecological Monographs*, *72*(3), 311–328. https://doi.org/10.2307/3100092

Tron, S., Laio, F., & Ridolfi, L. (2014). Effect of water table fluctuations on phreatophytic root distribution. *Journal of Theoretical Biology*, *360*, 102–108. https://doi.org/10.1016/j.jtbi.2014.06.035

Tron, S., Perona, P., Gorla, L., Schwarz, M., Laio, F., & Ridolfi, L. (2015). The signature of randomness in riparian plant root distributions. *Geophysical Research Letters*, *42*, 7098–7106. https://doi.org/10.1002/2015GL064857

How to cite this article: Stamer, M., Gurnell, A. M., & Bertoldi, W. (2024). Vertical root profiles of grey alder (*Alnus incana*) trees growing in highly disturbed river environments. *River Research and Applications*, *40*(6), 1001–1011. https://doi.org/10.1002/rra.4287